Development of the Tracking Compton/Pair-Creation Camera based on a Gaseous TPC and a Scintillation Camera

Kazuki Ueno[a], Toru Tanimori[a], Hidetoshi Kubo[a], Kentaro Miuchi[a], Shigeto Kabuki[a], Satoru Iwaki[a], Naoki Higashi[a], Joseph Parker[a], Shunsuke Kurosawa[a], Michiaki Takahashi[a], Tatsuya Sawano[a], Kojiro Taniue[a], Kiseki Nakamura[a], Hiroyuki Toyokawa[b], Atsushi Takada[c], Hironobu Nishimura[a], Kaori Hattori[a]

[a]*Kyoto University, Kitashirakawaoiwakecho, Sakyoku, Kyoto 606-8502, Japan*
[b]*National Institute of Advanced Industrial Science and Technology, Tsukuba, Ibaraki 305-8568, Japan*
[c]*Institute of Space and Astronautical Science, Japan Aerospace Exploration Agency, Yoshinodai, Sagamihara, Kanagawa 229-8510, Japan*

Abstract

We have evaluated the possibility of the Electron-Tracking Compton Camera (ETCC) to simultaneously operate as a pair-creation camera. The ETCC consists of a gaseous micro time projection chamber (micro-TPC) and a scintillation camera. Several prototypes of the camera were developed and their performance was studied. Because the micro-TPC can detect a large number of hit points along one charged particle track, has a good position resolution of about 0.2 mm, and uses the filling gas as the scattering material, the influence of multiple scattering is small. This makes the micro-TPC well-suited to detecting pair-creation events. We have examined the performance of a camera of size 10×10×15 cm^3, using the pair-creation mode in the energy range of 10 - 100 MeV. Using this camera, we performed a proof-of-principle experiment with laser inverse Compton gamma rays at the National Institute of Advanced Industrial Science and Technology (AIST), and we succeeded in tracking electron-positron pairs and in reconstructing 10 and 20 MeVgamma rays. In this paper, we report the fundamental performance of the gamma-ray camera with pair-creation mode.

Key words: Gamma-ray camera, Gaseous TPC, pair creation

1. Introduction

In the MeV gamma-ray astronomy, some observations with telescopes using Compton scattering or pair-creation, such as COMPTEL and EGRET onboard the Compton Gamma Ray Observatory (CGRO), have been successful [1, 2]. However, the detection sensitivity and the angular resolution in the energy range from sub-MeV to hundred MeV are worse than those of detectors in the X-ray, GeV, and TeV gamma-ray regions. In the low-energy region (sub-MeV – 10 MeV) where Compton scattering becomes dominant, the sensitivity is low since the telescope suffers from a large background. In the medium-energy region (10 – 100 MeV) where pair-creation becomes dominant, the angular resolution is much worse due to multiple scattering. Currently, there are no plans for an all sky survey with a satellite for the low and medium-energy regions. Although the Fermi satellite covers the medium-energy region, the angular resolution in the energy region below 100 MeV is still comparable to that of EGRET [3]. Thus, a gamma-ray camera with both improved detection sensitivity and angular resolution is desired.

We therefore have developed an Electron-Tracking Compton gamma-ray camera for the energy range of 0.1 – 10 MeV using a gaseous time projection chamber (micro-TPC) and a scintillation camera with the aim of conducting an all sky survey with a sensitivity 10 times better than that of COMPTEL, and with an angular resolution of ∼1 degree. Several prototypes with a detection volume of 10×10×10 cm^3 were developed, and their performances, with Compton mode only, were studied in the low-energy region [4, 5]. As a preliminary step toward an all sky survey, we are proceeding with balloon experiments. The first experiment in which we observed events of cosmic-diffuse and atmospheric gamma rays with Compton mode was done in 2006, and its results were reported in [6].

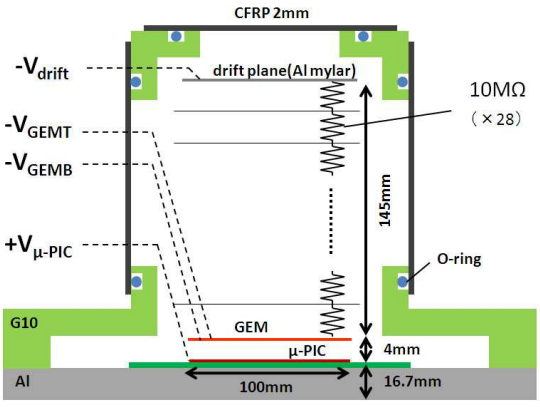

Figure 1: A schematic view of the micro-TPC.

Because the gaseous micro-TPC can detect a large number of hit points from one charged particle, has a good position resolution of about 0.2 mm, and uses the filling gas as the scattering material, the influence of multiple scattering is

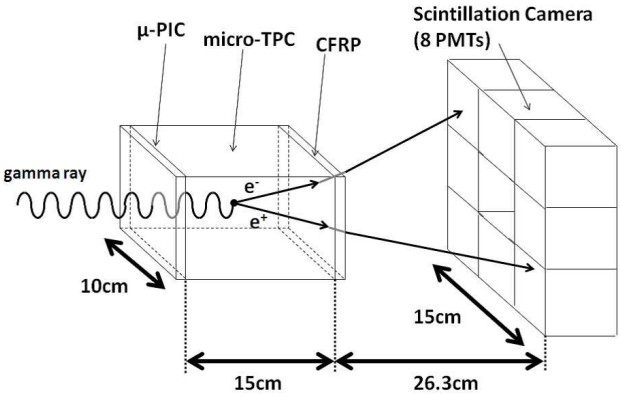

Figure 2: A schematic view of the gamma-ray camera for pair-creation mode.

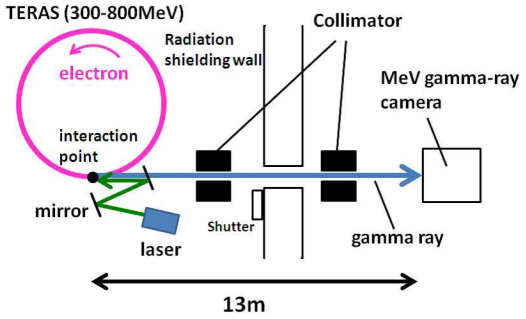

Figure 3: The experimental set up in the beam line.

small. This makes the micro-TPC well-suited for the detection of pair-creation events [7]. Thus, we have developed a camera of the same type as our Compton camera, with a size of $10\times10\times15$ cm^3 for the pair-creation mode. Then, using this camera, we performed a proof-of-principle experiment with laser inverse Compton gamma rays at the National Institute of Advanced Industrial Science and Technology (AIST), and we succeeded in tracking electron-positron pairs and in reconstructing 10 and 20 MeV gamma rays. In this paper, we present the results of the first experimental evaluation of the gamma-ray camera with pair-creation mode.

2. MeV gamma-ray camera for pair-creation mode

2.1. Instruments

For a proof-of-principle experiment in pair-creation mode, we constructed the same type of MeV gamma-ray camera as the one for Compton mode. The camera consists of two components. One is a gaseous micro-TPC with a volume of $10\times10\times15$ cm^3 (fiducial volume: $9\times9\times13$ cm^3) filled with an Ar and C_2H_6 (90:10) gas mixture at 1 atm. A schematic view of the micro-TPC is shown in Fig. 1. The micro-TPC detects the tracks of the electron-positron pairs created from the incoming gamma rays. Electrons released through ionization are multiplied by a micro pixel chamber (μ-PIC) [8] with an effective area of 10×10 cm^2 and a gas electron multiplier (GEM) [9]. The μ-PIC is our original gaseous two-dimensional imaging detector with a pixel pitch of 400 μm. The maximum stable gas gain of the μ-PIC is about 6000. However, a gas gain of 3×10^4 is required to obtain clear tracks of electron-positron pairs. Thus, a GEM, manufactured by Scienergy Co. Ltd. in Japan, was installed 4 mm above the μ-PIC as a pre-multiplication device for the micro-TPC. The thickness, hole diameter, and the hole pitch of the GEM are 50 μm, 70 μm, and 140 μm, respectively. A drift voltage of -5.53 kV was supplied to the drift plane ($V_{\rm drift}$ = 5.53 kV), creating a drift electric field of 0.32 kV/cm. The voltages of the top and bottom planes of the GEM were set to -830 V and -530 V ($V_{\rm GEMT}$ = 830 V, $V_{\rm GEMB}$ = 530 V), respectively. The μ-PIC voltage of 430 V was supplied to the anode electrodes ($V_{\mu-\rm PIC}$ = 430 V). We achieved the stable gas gain of 3.6×10^4 using these two devices, thus fulfilling the gas gain requirement. The position resolution of the micro-TPC was about 200 μm. The micro-TPC was installed in a vessel which consists of aluminum, Glass Fiber Reinforced Plastics (G10), and Carbon Fiber Reinforced Plastics (CFRP). In addition, a scintillation camera based on a 64 channel multi-anode position sensitive photomultiplier (PSPMT) coupled to GSO(Ce) scintillator arrays was positioned behind the micro-TPC. The effective area of this camera is 200 cm^2 corresponding to 8 PSPMTs. The position in the center of the scintillation camera was left free for the escaping gamma-ray beams. The details of the scintillation camera are described in [10]. We used the scintillation camera as the trigger detector in this setup. Fig. 2 shows the schematic view of the MeV gamma-ray camera for pair-creation mode.

2.2. Data acquisition system for tracking

A dedicated readout system for the micro-TPC was developed [11]. We have improved this system for tracking in order to increase the number of hit points. The output signals read by 256 anode-strips and 256 cathode-strips were digitized in amplifier-shaper-discriminator (ASD) chips [12], and then synchronized in a position encoder system with a 100 MHz clock. The resulting hit information was recorded by a VME memory board module. Each signal is given by a data set of (X_{max}, X_{min}, T) or (Y_{max}, Y_{min}, T), where X_{max} and X_{min} are the maximum and minimum positions of the anode strips, Y_{max} and Y_{min} are those of the cathode strips, and T is the clock counter. When the trigger signal from the scintillation camera is fed to the position encoder system, the clock counter starts and the data sets of X and Y are independently recorded during an 8 μsec time window.

3. First beam experiment

3.1. Experimental setup

We performed a proof-of-principle experiment with a laser inverse Compton gamma-ray beam at the National Institute of Advanced Industrial Science and Technology (AIST) [13]. A quasi-monochromatic gamma-ray beam was produced by the collision of laser photons with a 760 MeV electron beam accelerated in the storage ring TERAS. A Nd:YVO_4 laser with wavelengths of 1064 and 532 nm and a power of 1 W was used.

This system produced 10 and 20 MeV gamma rays, respectively. The experimental set up in the beam line is shown in Fig. 3. We aligned the gamma-ray camera on the beam axis. The distance between the gamma-ray camera and the point of origin of the beam was 13 m. In order to make the gamma-ray beam monochromatic and to focus it, lead collimators with a thickness of 20 cm and of 15 cm, and with a hole size of 1.8 mm diameter were put between the entrance of the beam and the gamma-ray camera. The diameter and the divergence of the beam at the micro-TPC were estimated to be 1.8 mm and 80 μrad, respectively.

3.2. Analysis

The tracks of the electron-positron pair were measured for the reconstruction of the pair-creation event. The direction of the incident gamma ray is given by

$$\vec{e}_{Inc} = \frac{E_e\vec{e}_e + E_p\vec{e}_p}{E_e + E_p}, \quad (1)$$

where, $\vec{e}_{Inc}$, $\vec{e}_e$, and $\vec{e}_p$ are the unit vectors of the incident gamma ray, of the electron, and of the positron, respectively. In this experiment, we could not measure the energy of the electron and of the positron, because the energy loss in the vessel wall was significant. Therefore, a simplification for Eq. (1) was needed, and the following simplified method was used:

$$\vec{e}_{Inc} \simeq \vec{e}_e + \vec{e}_p. \quad (2)$$

Fig. 4 shows typical tracks of an electron-positron pair measured in the micro-TPC. If the observed track pair had a large opening angle, it was fitted with two straight lines. Using the fitting lines, we calculated the vertex point and the unit vectors of the electron and of the positron. On the other hand, if the track pair had a small opening angle, it was fitted with one single straight line. For the current analysis, we selected events with the vertex point in the fiducial volume. In addition, for small angle events, we required that both the electron and the positron track were consistent with a "V" shape. To find "V" events, we used the selection parameter, R, defined by:

$$R = \frac{\sigma_d}{\sigma_u}, \quad (3)$$

where σ_d and σ_u were the root mean squares of the residual distributions from the single-line fit for hit points on the downstream side and on the upstream side of the center of gravity for the electron-positron track, respectively. If $R > 1$, the event was considered to be "V"-like. For the selected events, we calculated the unit vector of the incident gamma ray using Eq. (2), and we obtained images of gamma rays with 10 and with 20 MeV, respectively. Fig. 5 is the reconstructed image for 20 MeV gamma rays.

3.3. Results

Fig. 6 shows the θ-square distribution for 20 MeV gamma rays, where θ is the angular deviation between the measured and the real direction of the incident gamma rays. The angular resolution, given as the half-angle cone containing 68 % of

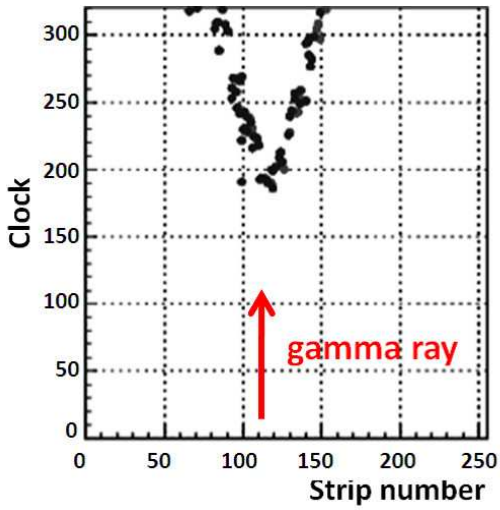

Figure 4: Typical tracks of an electron-positron pair.

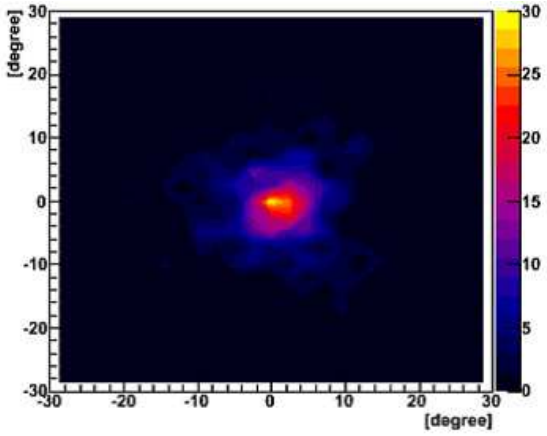

Figure 5: The obtained image for 20 MeV gamma rays.

all reconstructed events, was 7.7 degrees for the 20 MeV beam. In Fig. 7 the angular resolution is shown as a function of the energy of the incoming photons. For comparison, the angular resolutions of EGRET and MEGA [14] are also shown. We also simulated the ideal angular resolutions using Eq. (1) and Eq. (2), and these are shown in Fig. 7 as well. We can see that the measured angular resolutions are better by a factor of 1.5 compared to the results obtained with the silicon strip detector of MEGA. When we further develop the pixel readout system and improve the analysis method, the angular resolutions are expected to be close to the ideal ones using Eq. (2). Furthermore, we expect that by mounting the scintillation camera inside the vessel, we can make the resolution close to the ideal one using Eq. (1).

The detection efficiency was estimated as shown in Fig. 8. The gamma-ray flux was examined in a past experiment under similar conditions [15]. Using this result, we calculated the detection efficiency for 10 and 20 MeV gamma rays. The estimated detection efficiency for 20 MeV gamma rays was 1.4×10^{-5}. Compared with the probability of pair-creation in the micro-TPC, the obtained efficiency was smaller by an order

of magnitude. This is because the area covered by the scintillation camera was not large enough and the influence of the multiple scattering in the vessel was large. With the development of a larger scintillation camera and of an improved vessel, we expect to achieve a detection efficiency close to the pair-creation probability. Furthermore, we expect that the detection efficiency will be higher using a larger micro-TPC and selecting a gas with high Z, such as Xe.

Now, to obtain better angular resolutions and higher efficiency, we are improving the gamma-ray camera and the analysis method. If we make the gamma-ray camera with a volume of 1 m^3 filled with Xe gas, and if we mount the scintillation camera inside the vessel, the camera should achieve an effective area of about 100 cm^2 and an angular resolution of less than 1 degree. Those performances are similar to EGRET and Fermi at energies below 100 MeV.

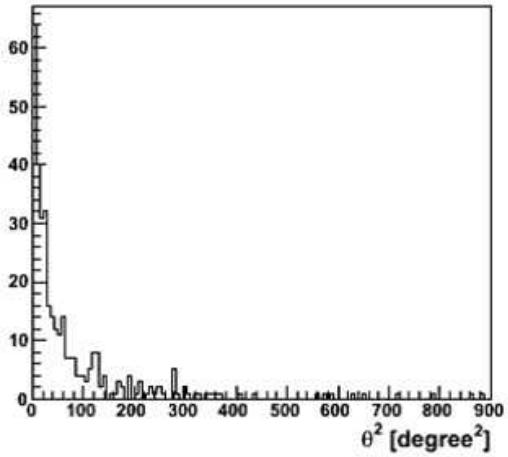

Figure 6: The distribution of the angular deviation between the measured and the real origin for 20 MeV gamma rays.

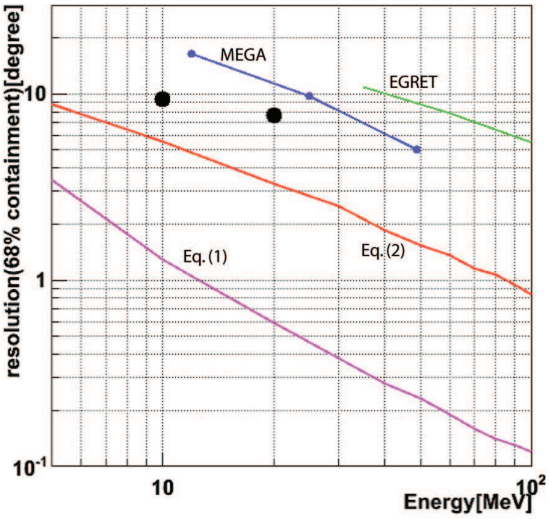

Figure 7: The angular resolution of the gamma-ray camera (68 % containment) as a function of the photon energy. The filled circles represent the measured values. For comparison, the resolutions of EGRET, of MEGA[14], and the resolutions simulated with Eq. (1) and Eq. (2) are also shown.

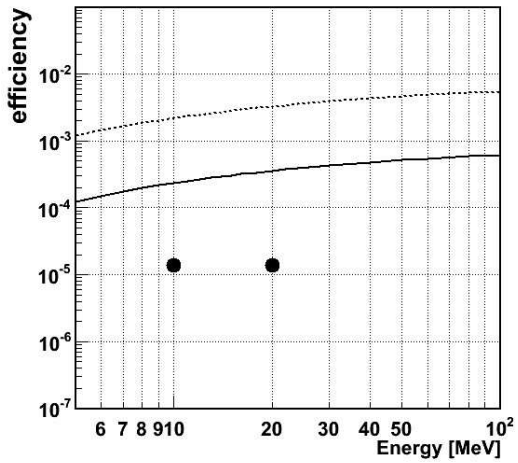

Figure 8: The estimated detection efficiency of the gamma-ray camera (filled circles). The solid line and the dashed line are the probabilities of pair-creation in the micro-TPC with an Ar and C_2H_6 gas mixture (90:10) and with Xe, respectively.

4. Summary

We have evaluated the possibility of our Electron-Tracking Compton Camera (ETCC) to simultaneously operate as a pair-creation camera. We performed a proof-of-principle experiment with a laser inverse Compton gamma-ray beam, using the gamma-ray camera with a volume of 10×10×15 cm^3 (fiducial volume: 9×9×13 cm^3) in pair-creation mode. The tracks of the electron-positron pairs were detected, and the incident gamma rays of 10 and 20 MeV were reconstructed. We obtained an angular resolution of 7.7 degrees for 20 MeV incident photons, and we estimated a detection efficiency of 1.4×10^{-5}.

Acknowledgments

This work is supported by the Global COE Program "The Next Generation of Physics, Spun from Universality and Emergence" and JSPS Research Fellowships for Young Scientists.

References

[1] V. Schönfelder et al., Astrophys. J. Suppl. Ser. 86 (1993) 657.
[2] G. Kanbach et al., Space. Sci. Reviews. 49 (1998) 69.
[3] A. A. Moiseev, Nucl. Instr. and Meth. A 588 (2008) 41.
[4] R. Orito et al., Nucl. Instr. and Meth. A 525 (2004) 107.
[5] A. Takada et al., Nucl. Instr. and Meth. A 546 (2005) 258.
[6] A. Takada et al., JSPJ 78 (2009) 161.
[7] R. Orito et al., Nucl. Instr. and Meth. A 513 (2003) 408.
[8] A. Ochi et al., Nucl. Instr. and Meth. A 471 (2001) 264.
[9] F. Sauli, Nucl. Instr. and Meth. A 386 (1997) 531.
[10] S. Kurosawa et al., IEEE Trans. Nucl. Sci. 56 (2009) 3779.
[11] H. Kubo et al., IEEE Nucl. Sci. Symp. Conf. Rec. N14-30 (2005).
[12] O. Sasaki, M. Yoshida, IEEE Trans. Nucl. Sci. 46 (1999) 1871.
[13] H. Ohgaki, H. Toyokawa, K. Kudo, N. Takeda, T. Yamazaki, Nucl. Instr. and Meth. A 455 (2000) 54.
[14] G. Kanbach et al., Nucl. Instr. and Meth. A 541 (2005) 310.
[15] H. Toyokawa et al., Nucl. Instr. and Meth. A 608 (2009) 41.